



Fatigue crack propagation prediction of a pressure vessel mild steel based on a strain energy density model

P. J. Huffman

John Deere, One John Deere Place, Moline, IL 61265, USA

huffman.peter.j@gmail.com

J. Ferreira, J.A.F.O. Correia, A.M.P. De Jesus

INEGI, Faculty of Engineering, University of Porto, Rua Dr. Roberto Frias, 4200-465 Porto, Portugal

em12236@fe.up.pt, jacorreia@inegi.up.pt, ajesus@fe.up.pt

http://orcid.org/0000-0002-4148-9426, http://orcid.org/0000-0002-1059-715X

G. Lesiuk

Faculty of Mechanical Engineering, Department of Mechanics, Material Science and Engineering, Wrocław University of Science and Technology, Smoluchowskiego 25, 50-370 Wrocław, Poland

Grzegorz.Lesiuk@pwr.edu.pl, https://orcid.org/0000-0003-3553-6107

F. Berto

Department of Industrial and Mechanical Design, Norwegian University of Science and Technology, Norway

berto@gest.unipd.it, filippo.berto@ntnu.no, http://orcid.org/0000-0002-4207-0109, http://orcid.org/0000-0002-0591-0754

A. Fernández-Canteli

Department of Construction and Manufacturing Engineering, Univ. of Oviedo, 33203 Gijón, Spain

afc@uniovi.es, http://orcid.org/0000-0001-8071-9223

G. Glinka

Department of Mechanical Engineering, University of Waterloo, 200 Univ. Avenue West, Waterloo, ON, N2L 3G1, Canada

gggreg@uwaterloo.ca, http://orcid.org/0000-0001-8452-8803

ABSTRACT. Fatigue crack growth (FCG) rates have traditionally been formulated from fracture mechanics, whereas fatigue crack initiation has been empirically described using stress-life or strain-life methods. More recently, there has been efforts towards the use of the local stress-strain and similitude concepts to formulate fatigue crack growth rates. A new model has been developed which derives stress-life, strain-life and fatigue crack growth rates from strain energy density concepts. This new model has the advantage to predict an intrinsic stress ratio effect of the form $\sigma_{ar} = (\sigma_{amp})^\gamma \cdot (\sigma_{max})^{(1-\gamma)}$, which is

OPEN ACCESS

Citation: Huffman, P.J., Ferreira, J., Correia, J.A.F.O., De Jesus, A.M.J., Lesiuk, G., Berto, F., Glinka, G., Fernández-Canteli, A., Fatigue crack propagation prediction of a pressure vessel mild steel based on a strain energy density model, *Frattura ed Integrità Strutturale*, 42 (2017) 74-84.

Received: 16.06.2017



dependent on the cyclic stress-strain behaviour of the material. This new fatigue crack propagation model was proposed by Huffman based on Walker-like strain-life relation. This model is applied to FCG data available for the P355NL1 pressure vessel steel. A comparison of the experimental results and the Huffman crack propagation model is made.

Accepted: 21.06.2017

Published: 01.10.2017

Copyright: © 2017 This is an open access article under the terms of the CC-BY 4.0, which permits unrestricted use, distribution, and reproduction in any medium, provided the original author and source are credited.

KEYWORDS. Fatigue Crack Growth; Strain Energy; Unigrow Model; Pressure Vessel Steel.

INTRODUCTION

Fatigue crack initiation, usually modelled by strain-life or stress-life, has traditionally been considered to be a separate physical phenomenon from fatigue crack propagation. However, some more recent models of fatigue crack growth have been based on the assumption that each crack growth increment is physically similar to the initiation process. That is, the individual crack growth increments are successive initiations of the crack locally at the crack tip [1-4]. Such models consider fatigue crack initiation and propagation to be physically similar, and they can be used in a unified approach to calculate total fatigue life as the sum of initiation and propagation [5-7].

Some authors, as Glinka [2], Peeker and Niemi [3], Noroozi et al. [4,6,7], Hurley and Evans [5] developed approaches to represent fatigue crack propagation using local fatigue models based on strain parameters. Glinka was one of the precursors to describe the fatigue crack propagation modelling using a strain-based fatigue relation [2].

Similarly, the model proposed by Peeker and Niemi [3] allowed the near threshold fatigue crack propagation data and the stable crack growth to be described. For the near threshold fatigue crack propagation, the authors derived analytical relations which are functions of the strain-life relation constants.

Hurley and Evans [5] proposed the use of an elastoplastic finite element analysis to compute the process zone and using the Walker-like strain correlated directly with the fatigue life from experimental data thru a power relation to correlate with the fatigue crack increment.

Other authors, such as, Correia et al. [8-14] and Hafezi et al. [15] used the strain and SWT fatigue local relations [16], based on UniGrow model [4,6,7] to predict the fatigue crack propagation using the numerical analysis to obtain residual stresses distribution. Correia et al. [9,17,18] proposed a procedure to derive probabilistic S-N-R fields for notched structural details or mechanical components, which is based on the UniGrow model and numerical analysis aiming at computing the elastoplastic stresses and strains at process zone ahead the crack tip. Alternatively, analytical methods such as the ones proposed by Neuber [19] and Moftakhar et al. [20] may be applied to perform the elastoplastic analysis taking into account the elastic stress/strain fields computed around the crack tip, using available Linear Elastic Fracture Mechanics solutions [4,20,21].

Recently, Huffman [1] suggested new developments related with the fatigue crack propagation modelling using strain energy density-based model. Fatigue evaluation of notched details based on unified local probabilistic approaches was also proposed by Huffman [22] considering the Walker-like strain-life relation in conjunction with the probabilistic model proposed by Castillo and Fernández-Canteli [23].

In present research, the Huffman crack propagation model is applied to the P355NL1 pressure vessel steel and a comparison with experimental results is made.

OVERVIEW OF LOCAL STRESS/STRAIN APPROACHES

Fatigue crack growth modelling like the Paris law relation, uses Linear-Elastic Fracture Mechanics (LEFM) to describe cracking driving forces. Local approaches, however, explicitly consider stresses and strains near the crack tip, and associate those with the stress intensity factors. Using the assumption that the stresses or strains near the crack tip are related to fatigue crack growth in the same way that global stresses and strains are related to stress-life and strain-life, an association can be made between damage parameters, such as the SWT damage parameter [16] or the damage parameter introduced by Huffman [1] and the fatigue crack growth.



The latter approach assumes that stress-life, strain-life, and fatigue crack growth are all different expressions of the same phenomenon which is directly associated with the cyclic stress-strain behaviour. According to that work, the stress life, strain life, and fatigue crack growth rate can all be expressed in terms of material parameters. The damage parameter in this case is

$$\left(\frac{U_e}{U_d \rho_c} \right) \left(\frac{U_p^*}{U_d \rho_c} \right) = D = \frac{2N}{2N_f} \quad (1)$$

where U_e is the elastic strain energy density and U_p^* is the complimentary plastic strain energy density, both from integrating the cyclic Ramberg-Osgood stress-strain curve [24], ρ_c is the critical dislocation density, U_d is the dislocation strain energy, and D is the damage corresponding to those strain energy inputs. The dislocation strain energy is calculated as

$$U_d = \left(\frac{E}{2(1+\nu)} \right) \|\vec{b}\|^2 \quad (2)$$

where ν is the Poisson's ratio and \vec{b} is the Burger's vector. The damage stress based is then defined as

$$\left(\frac{2}{U_d^2 \rho_c^2} \right) \left(\frac{n'}{1+n'} \right) \left(\frac{1}{K'} \right) (\sigma_{\max}^2) (\sigma_a)^{\frac{1+n'}{n'}} = D = \frac{1}{2N_f} \quad (3)$$

The Morrow constants can be calculated as follows.

$$\sigma_f' = E \left(\frac{2}{U_d^2 \rho_c^2} \left(\frac{1}{K'} \right)^{1/n'} \left(\frac{n'}{1+n'} \right) E^{(1+2n')n'} \right)^{\frac{n'}{1+3n'}} \quad (4)$$

where E is the elastic modulus, K' is the cyclic strength coefficient, n' is the cyclic strain hardening exponent and σ_f' is the fatigue strength coefficient. In this model, K' and n' come from fitting the cyclic stress and strain amplitude to the Ramberg-Osgood equation.

$$b = \frac{-n'}{1+3n'} \quad (5)$$

where b is the fatigue strength exponent.

$$\varepsilon_f' = E \left(\frac{2(K')^3}{U_d^2 \rho_c^2 E} \left(\frac{n'}{1+n'} \right) \right)^{\frac{1}{1+3n'}} \quad (6)$$

where ε_f' is the fatigue ductility coefficient

$$c = \frac{-1}{1+3n'} \quad (7)$$

where c is the fatigue ductility exponent.

The product of Eq. (3) by Δa , results a method for calculating the fatigue crack growth rates:



$$\left(\frac{\Delta a}{U_d^2 \rho_c^2} \right) \left(\frac{n'}{1+n'} \right) \left(\frac{1}{K'} \right) (\sigma_{\max}^2) (\sigma_a)^{\frac{1+n'}{n'}} = \frac{\Delta a}{N_f - 0} \approx \frac{da}{dN} \quad (8)$$

where the stresses are the local stresses at the crack tip. This can be related to the stress intensity factor to yield a formula similar to what is used by Noroozi et al. [4,6,7] or alternatively to use the procedure to obtain the fatigue crack growth driving force, $\Delta\kappa$, considering a finite element analysis to compute residual stress intensity factor, K_r proposed by Correia et al. [8-14] and Hafezi et al. [15],

$$\frac{da}{dN} = C (\Delta\kappa)^\gamma \quad (9)$$

where C is the fatigue crack growth rate coefficient, γ is the fatigue crack growth rate exponent, and $\Delta\kappa$, the fatigue crack growth driving force.

$$\Delta\kappa = K_{\max}^p (\Delta K)^{1-p} \quad (10)$$

where

$$p = \frac{2n'}{1+3n'} \quad (11)$$

The fatigue crack growth rate exponent can be shown to be

$$\gamma = \frac{2+6n'}{1+n'} = \frac{-2}{b+c} \quad (12)$$

For predominantly plastic stresses at the crack tip, the fatigue crack growth rate coefficient under the same conditions is given by,

$$C = \left(\frac{\Delta a}{U_d^2 \rho_c^2} \right) \left(\frac{n'}{1+n'} \right) (K')^{\frac{2}{1+n'}} (E)^{-\left(\frac{4n'+2}{n'+1}\right)} \left(\frac{1}{2} \right)^{\frac{1}{n'}} \left(\frac{1}{2\pi\alpha} \right)^{\frac{1+3n'}{1+n'}} \quad (13)$$

APPLICATION OF THE STRAIN ENERGY DENSITY APPROACH TO FCG DATA

Experimental fatigue crack growth data

The P355NL1 steel is a pressure vessel steel and was selected to apply the strain energy density approach to fatigue crack growth data. The mechanical properties of this steel were collected from the references [9,12,25,26]. In this sub-section the monotonic strength data, the cyclic elastoplastic fatigue data and the fatigue crack growth data obtained for the P355NL1 steel [9,12,25,26] are presented.

The elastic and monotonic tensile properties for this steel under investigation, such as the Young modulus, E , Poisson ratio, ν , the ultimate tensile strength, f_u , upper yield stress, f_y , monotonic strain hardening coefficient, K , and monotonic strain hardening exponent, n , are shown in Tab. 1. Also, in Tab. 1, the Ramberg-Osgood parameters are presented including the cyclic strain hardening coefficient, K' , and the cyclic strain exponent, n' .

The strain-life behaviour of the P355NL1 steel was evaluated through fatigue tests of smooth specimens, carried out under strain-controlled conditions, according to the ASTM E606 standard [27]. Two series of specimens are tested under distinct strain ratios, $R_e=0$ and -1, 19 and 24 specimens, respectively. The cyclic Ramberg-Osgood [24] and Morrow [28-30] strain-life parameters of the P355NL1 steel are summarized in Tab. 2, for the conjunction of both strain ratios. The Morrow strain-life parameters, such as, the fatigue ductility coefficient, ε_f' , the fatigue ductility exponent, c , the fatigue strength coefficient, σ_f' , and the fatigue strength exponent, b , were collected in references [9,12,25,26].



Material	E (GPa)	ν	f_f (MPa)	f_u (MPa)	K (MPa)	n	K' (MPa)	n'
P355NL1	205.0	0.275	361.99	361.99	611.49	0.063	948.35	0.1533

Table 1: Elastic, monotonic tensile and Ramberg-Osgood properties for the P355NL1 steel.

Material	σ_f^* (MPa)	b	ε_f^*	c
P355NL1	1005.50	-0.1033	0.3678	-0.5475

Table 2: Morrow constants for the P355NL1 steel for strain R-ratios, $R_\epsilon=-1 + R_\sigma=0$.

The experimental results of the fatigue crack growth rates of the investigated material are also evaluated for several stress R-ratios, using CT specimens, following the recommendations of the ASTM E647 standard [31]. The CT specimens of P355NL1 steel are defined with a width, $W=40\text{mm}$ and a thickness, $B=4.5\text{mm}$ [9,12,25,26]. The tests were performed in air, at room temperature, under a sinusoidal waveform at a maximum frequency of 20 Hz. In Fig. 1, the crack growth data derived for the P355NL1 steel, for three tested stress ratios, $R_\sigma=0.0$, $R_\sigma=0.5$ and $R_\sigma=0.7$, are shown. The crack propagation rates are only slightly influenced by the stress ratio. Higher stress ratios provide higher crack growth rates [9,12,25,26].

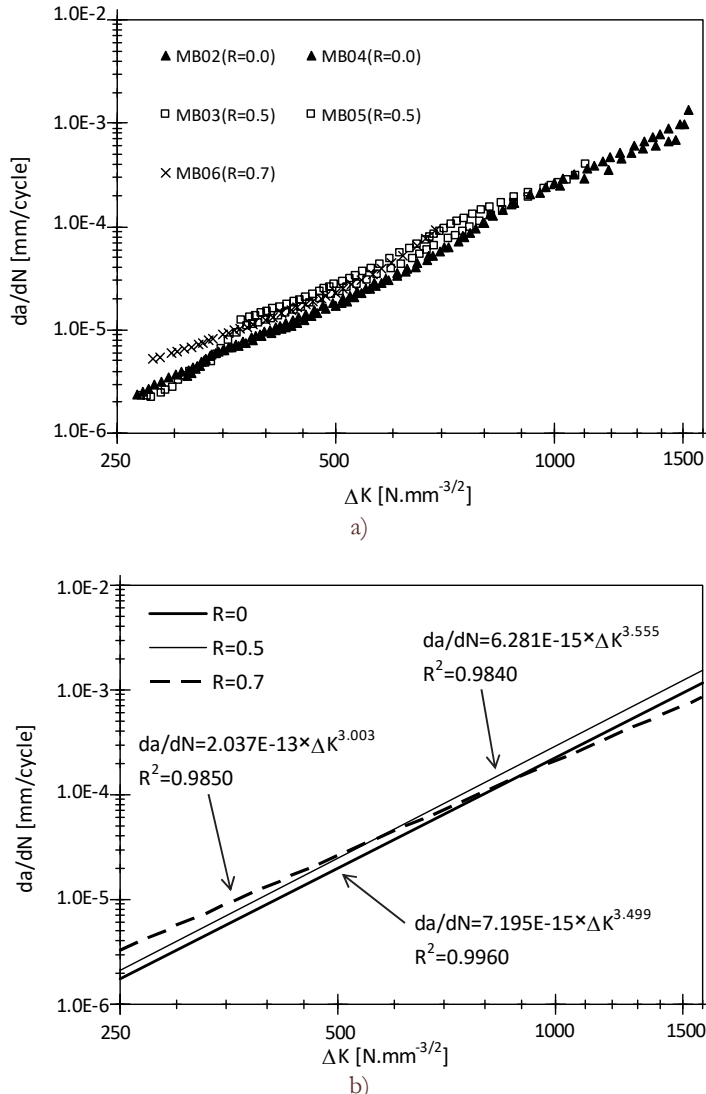


Figure 1: Fatigue crack growth data of the P355NL1 steel: a) Experimental data; b) Paris correlations for each stress R-ratio.



Brief description of the numerical analysis

In this sub-section, a brief description of the numerical analysis of the CT specimens performed by Correia et al. [9,10,13] is presented. This author developed two dimensional numerical models of the CT specimens using non-linear elastoplastic finite element analysis. Fig. 2 illustrates the finite element mesh of the CT specimen along with the respective boundary conditions. One half of the geometry is modelled, taking advantage of the existing symmetry. 2D plane stress elements are used since the specimens' thickness is relatively small ($B=4.5\text{mm}$). Quadratic triangular elements (6-noded elements) are selected and applied with a full integration formulation. The pin loading applied to the CT specimens is simulated with a rigid-to-flexible frictionless contact, the pin being modelled as a rigid circle controlled by a pilot node. All numerical simulations are carried out using the ANSYS® 12.0 code [32]. The 6-noded plane element adopted in the FE (finites elements) analyses is the PLANE181 element available in the ANSYS® 12.0 code library. The contact and target elements used in the pin-loading simulation are, respectively, the CONTA172 and TARGE169 elements available in ANSYS® 12.0 code [32]. A parametric model is built using the APDL language. The surface of the holes is modelled as flexible, using CONTA172 elements. The Augmented Lagrange contact algorithm is used. The associative Von Mises (J2) yield criterion with multilinear kinematic hardening is used to model the plastic behaviour. The multilinear kinematic hardening uses the Besseling model, also called the sublayer or overlay model, so that the Bauschinger effect is included. The plasticity model was fitted to the stabilized or half-life pseudo stabilized cyclic curve of the materials. The plasticity model is fitted to the cyclic curve of the material using the cyclic Ramberg-Osgood properties of the Tab. 1.

The finite element model is applied to perform elastic and elastoplastic stress analyses. One important assumption of the Huffman fatigue crack propagation model consists in applying the compressive residual stresses that are computed ahead of the crack tip, in the crack faces, in a symmetric way with respect to the normal to crack face that passes thru the crack tip. The residual stresses distribution was estimated using the numerical simulation proposed by Correia et al. [9]. The resulting residual stress intensity factor, K_r , was computed using the weight function method [33], for each of the stress ratios covered by the testing program.

Fig. 3 presents the residual stress intensity factor range [12] as a function of the applied stress intensity factor range, obtained with the numerical analysis, which is consistent with the analytical analysis followed in the UniGrow model published in the literature. A very high linear correlation between the residual stress intensity factor and the applied stress range is verified, for each stress R-ratio. This linear relation agrees with the proposition by Noroozi et al. [4], based on analytical analysis. The numerical solution, for the residual stresses, is adopted in the crack propagation prediction using Huffman fatigue crack propagation model [1].

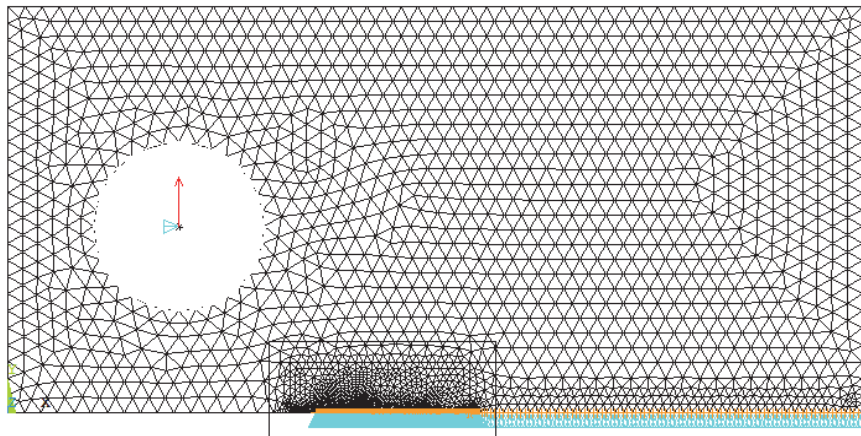
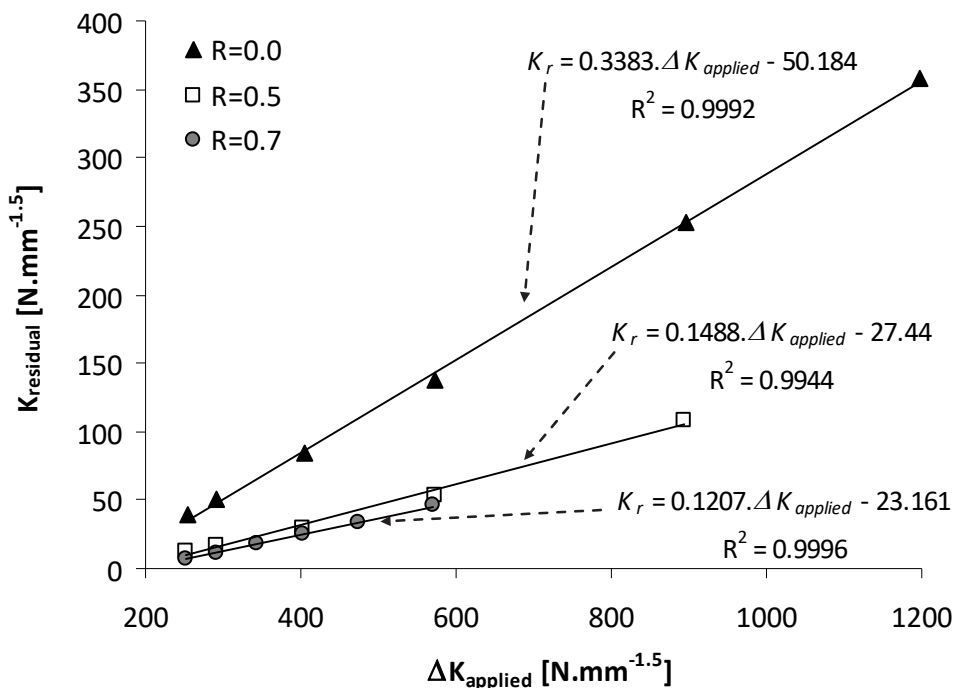


Figure 2. Finite element mesh of the CT specimen [9].

Application and results

This sub-section presents the application of the strain energy density approach to fatigue crack propagation data of the P355NL1 pressure vessel steel. From the application of this model, the Morrow and fatigue crack growth constants, as well as, the strain-life and stress-life curves are evaluated. The fatigue crack propagation model based on the strain energy density approach requires the calibration of model parameters, such as, the critical dislocation density, ρ_c , crack increment, Δa , and distance from the crack tip, x .

Figure 3. Residual stress intensity factor as a function of the $\Delta K_{\text{applied}}$ for the CT geometry.

The Morrow constants resulting from Eqs. (4)-(7) can be seen in Tab. 3. These constants, estimated using the strain energy density approach, are similar to those obtained by fitting the Coffin-Manson and Morrow relation. In this way, it is demonstrated that the Huffman fatigue crack propagation model leads to good results. The fatigue crack growth rate constants are shown in Tab. 4, as well as the critical dislocation density for the material. These FCG rate constants were estimated using the strain energy density approach related to the stress intensity factor used by Noroozi et al. [4] and considering the residual stresses distribution obtained numerically (proposed by Correia et al. [9]).

Material	$\sigma_f' \text{ (MPa)}$	b	ε_f'	c
P355NL1	959	-0.105	1.08	-0.685

Table 3: Morrow constants for the P355NL1 calculated as per Eqs. (4)-(7).

Material	$\rho_c \text{ (m/m}^3)$	$\Delta a \text{ (m)}$	$x \text{ (m)}$
P355NL1	7.0×10^{-15}	4.5E-3	3.0E-5

Table 4: Fatigue crack growth rate constants from Eq. (8).

The stress-life and strain-life curves, and fatigue crack growth rates calculated from the strain energy based damage model are presented, respectively, in the Figs. 4, 5 and 6. A good agreement between the experimental strain-life test results and stress- and strain-life curves estimated using the strain energy density approach is verified. A good agreement can be considered between the experimental FCG results and the results obtained on the basis of the Huffman fatigue crack propagation model for the stress R-ratio equal to 0 and the set of experimental FCG results for all stress R-ratios. This model shows to be very conservative for the stress R-ratios equal to 0.5 and 0.7, describing a possible mean stress effect that is not verified for this material. The critical dislocation density and basic fatigue crack growth rates constants (Tab. 4) for the P355NL1 steel are similar when compared with others materials of identical mechanical properties.

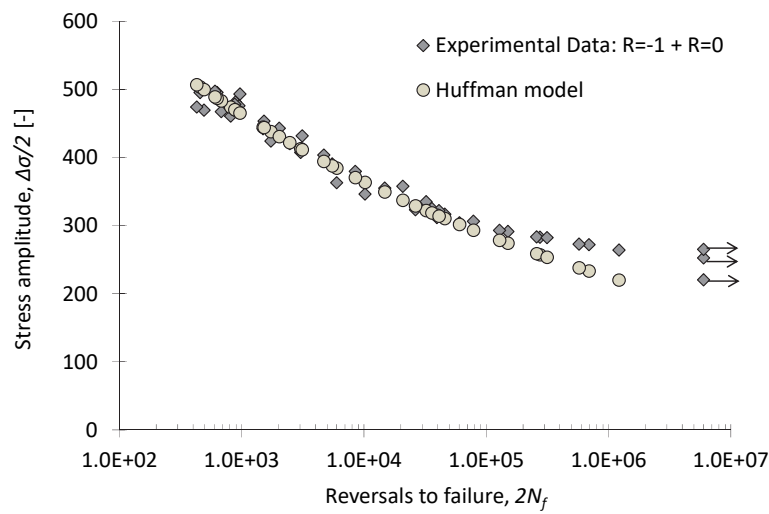


Figure 4. Stress-life curve of the P355NL1 steel, per reference [1].

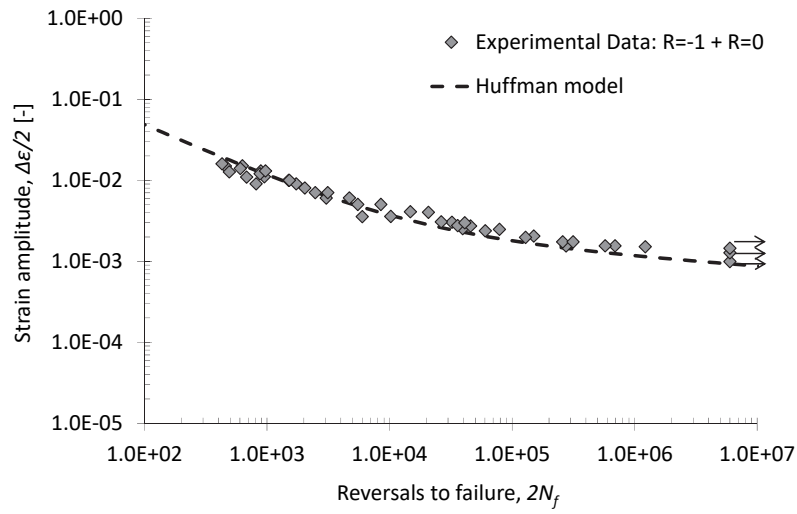
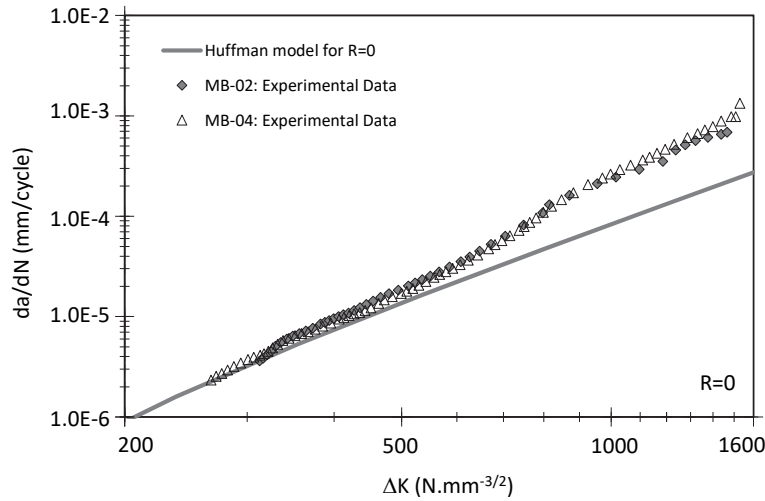


Figure 5. Strain-life curve of the P355NL1 steel, per reference [1].



a)

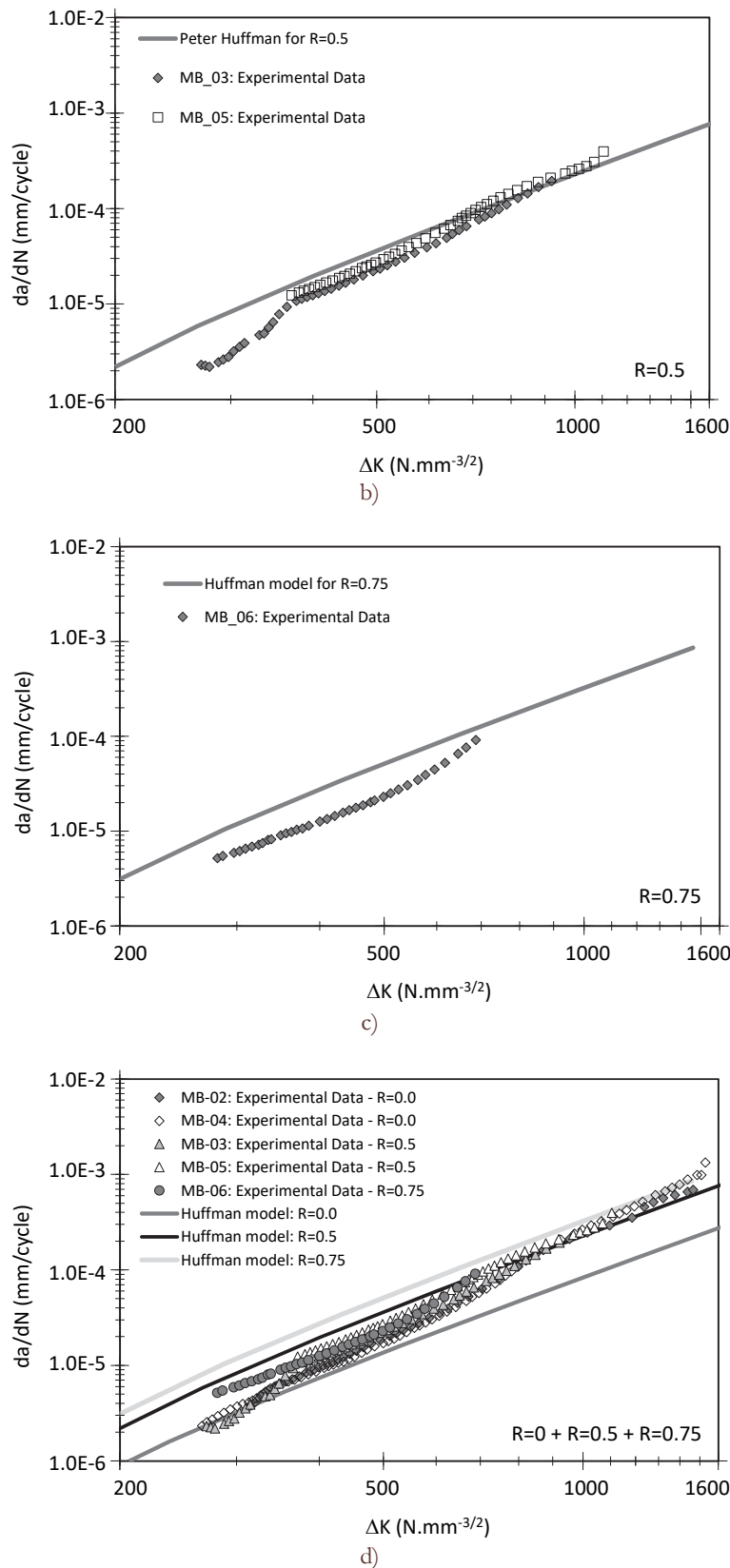


Figure 6. Fatigue crack growth rate of P355NL1 steel obtained using the Huffman model, as per reference [1]: a) R=0; b) R=0.5; c) R=0.75; d) R=0 + R=0.5 + R=0.75.



CONCLUSIONS

The Huffman fatigue crack initiation and propagation model based on a strain energy based damage model can be used to predict the stress-life and strain-life curves, as well as the fatigue crack propagation rates in Paris' law regime, along with the corresponding stress ratio effect.

A good agreement between the experimental strain-life results and Huffman analytical stress- and strain-life curves is verified. The model is able to obtain fatigue local relations for other fatigue damage parameters, such as SWT fatigue damage parameter.

The application of the Huffman model to the fatigue crack propagation data of the P355NL1 steel proved to be promising. Some aspects related with the mean stresses and stress R-ratios effects have to be improved in order to correctly describe the fatigue crack growth behaviour of the material under consideration. A comparison with other models of fatigue crack propagation based on fatigue local approaches should be made, such as UniGrow model using Neuber analytical approaches or numerical modelling to obtain the residual stresses distribution.

A unified two-stage fatigue approach using the Huffman fatigue crack initiation and propagation model applied to the structural details can be suggested.

ACKNOWLEDGEMENTS

The authors acknowledge the Portuguese Science Foundation (FCT) for the financial support through the postdoctoral Grant SFRH/BPD/107825/2015. The authors gratefully acknowledge the funding of SciTech: Science and Technology for Competitive and Sustainable Industries, R&D project cofinanced by Programa Operacional Regional do Norte (NORTE2020), through Fundo Europeu de Desenvolvimento Regional (FEDER).

REFERENCES

- [1] Huffman, P.J., A strain energy based damage model for fatigue crack initiation and growth, *International Journal of Fatigue*, 88 (2016) 197–204.
- [2] Glinka, G., A notch stress-strain analysis approach to fatigue crack growth, *Engineering Fracture Mechanics*, 21 (1985) 245–261.
- [3] Peeker, E., Niemi, E., Fatigue crack propagation model based on a local strain approach, *Journal of Constructional Steel Research*, 49 (1999) 139–155.
- [4] Noroozi, A.H., Glinka, G., Lambert, S., A two parameter driving force for fatigue crack growth analysis, *International Journal of Fatigue*, 27 (2005) 1277-1296.
- [5] Hurley, P.J., Evans, W.J., A methodology for predicting fatigue crack propagation rates in titanium based on damage accumulation, *Scripta Materialia*, 56 (2007) 681–684.
- [6] Noroozi, A.H., Glinka, G., Lambert, S., A study of the stress ratio effects on fatigue crack growth using the unified two-parameter fatigue crack growth driving force, *International Journal of Fatigue*, 29 (2007) 1616-1633.
- [7] Noroozi, A.H., Glinka, G., Lambert, S., Prediction of fatigue crack growth under constant amplitude loading and a single overload based on elasto-plastic crack tip stresses and strains, *Engineering Fracture Mechanics*, 75 (2008) 188-206.
- [8] Correia, J.A.F.O., De Jesus, A.M.P., Fernández-Canteli, A., A procedure to derive probabilistic fatigue crack propagation data, *International Journal of Structural Integrity*, 3(2) (2012) 158–183.
- [9] Correia, J.A.F.O., De Jesus, A.M.P., Fernández-Canteli, A., Local unified model for fatigue crack initiation and propagation: application to a notched geometry, *Engineering Structures*, 52 (2013) 394–407.
- [10] Correia, J.A.F.O., An integral probabilistic approach for fatigue lifetime prediction of mechanical and structural components, Ph.D. Thesis, University of Porto, (2014) 382.
- [11] Correia, J.A.F.O., De Jesus, A.M.P., Fernández-Canteli, A., Calçada, R.A.B., Modelling probabilistic fatigue crack propagation rates for a mild structural steel, *Frattura ed Integrità Strutturale*, 31 (2015) 80-96.
- [12] De Jesus, A.M.P., Correia, J.A.F.O., Critical assessment of a local strain-based fatigue crack growth model using experimental data available for the P355NL1 steel, *Journal of Pressure Vessel Technology*, 135(1) (2013) 011404-1–0114041-9.



- [13] Correia, J.A.F.O., De Jesus, A.M.P., Moreira, P.M.G.P., Calçada, R.A.B., Fernández-Canteli, A., Fatigue Crack Propagation Rates Prediction Using Probabilistic Strain-Based Approaches, Chapter 11, pp. 245-273, in: Fracture Mechanics – Properties, Patterns and Behaviours, Lucas Alves (Ed.), (2016).
- [14] Hafezi, M.H., Abdullah, N.N., Correia, J.A.F.O., De Jesus, A.M.P., An assessment of a strain-life approach for fatigue crack growth, *International Journal of Structural Integrity*, 3(2) (2012) 344–376.
- [15] Correia, J.A.F.O., De Jesus, A.M.P., Ribeiro, A.S., Strain-based approach for fatigue crack propagation simulation of the 6061-T651 aluminum alloy, *International Journal of Materials and Structural Integrity*, (2017, in press).
- [16] Smith, K.N., Watson, P., Topper, T.H., A Stress-Strain Function for the Fatigue of Metals, *Journal of Materials*, 5(4) (1970) 767-778.
- [17] Sampayo, L.M.C.M.V., Monteiro, P.M.F., Correia, J.A.F.O., Xavier, J.M.C., De Jesus, A.M.P., Fernandez-Canteli, A., Calçada, R.A.B., Probabilistic S-N field assessment for a notched plate made of puddle iron from the Eiffel bridge with an elliptical hole, *Procedia Engineering*, 114 (2015) 691 – 698.
- [18] Raposo, P., Correia, J.A.F.O., De Jesus, A.M.P., Calçada, R.A.B., Lesiuk, G., Hebdon, M., Fernández-Canteli, A., Probabilistic fatigue S-N curves derivation for notched components, *Frattura ed Integrità Strutturale*, (2017, in press).
- [19] Neuber, H., Theory of stress concentration for shear-strained prismatic bodies with arbitrary nonlinear stress-strain law. *Trans. ASME Journal of Applied Mechanics*, 28 (1961) 544–551.
- [20] Moftakhar A, Buczynski A, Glinka G. Calculation of elasto-plastic strains and stresses in notches under multiaxial loading. *International Journal of Fracture*, 70 (1995) 357-373.
- [21] Reinhard W, Moftakhar A, Glinka G. An Efficient Method for Calculating Multiaxial Elasto-Plastic Notch Tip Strains and Stresses under Proportional Loading. *Fatigue and Fracture Mechanics*, Vol. 27, ASTM STP 1296, R.S. Piascik, J.C. Newman, N.E. Dowling, Eds., American Society for Testing and Materials, (1997) 613-629.
- [22] Huffman, P., Correia, J.A.F.O., Mikheevskiy, S., De Jesus, A.M.P., Cicero, S., Fernández-Canteli, A., Berto, F., Glinka, G., Fatigue evaluation of notched details based on unified local probabilistic approaches, *International Symposium on Notch Fracture (ISNF2017)*, Santander, Spain, (2017).
- [23] Castillo, E., Fernández-Canteli, A., A Unified Statistical Methodology for Modeling Fatigue Damage, Springer, 2009.
- [24] Ramberg, W., Osgood, W.R., Description of the stress-strain curves by the three parameters, NACA TN-902, National Advisory Committee for Aeronautics, (1943).
- [25] De Jesus, A.M.P., Ribeiro, A.S., Fernandes, A.A., Influence of the submerged arc welding in the mechanical behaviour of the P355NL1 steel—Part II: Analysis of the Low/High Cycle Fatigue Behaviours, *J. Mater. Sci.*, 42 (2007) 5973–5981.
- [26] Correia, J.A.F.O., De Jesus, A.M.P., Moreira, P.M.G.P., Tavares, P.J., Crack closure effects on fatigue crack propagation rates: application of a proposed theoretical model, *Advances in Materials Science and Engineering*, (2016) 3026745.
- [27] ASTM – American Society for Testing and Materials. ASTM E606-92: standard practice for strain controlled fatigue testing. In: Annual book of ASTM standards, part 10; (1998) 557–571.
- [28] Coffin, L.F., A study of the effects of the cyclic thermal stresses on a ductile metal, *Trans ASME*, 76 (1954) 931–950.
- [29] Manson, S.S., Behaviour of materials under conditions of thermal stress, NACA TN-1170, National Advisory Committee for Aeronautics, Report 1170, (1954) 591–630.
- [30] Morrow, J.D., Cyclic plastic strain energy and fatigue of metals, *Int Frict Damp Cyclic Plast ASTM STP*, 378 (1965) 45–87.
- [31] ASTM—American Society for Testing and Materials. ASTM E647: standard test method for measurement of fatigue crack growth rates. In: Annual book of ASTM Standards, vol. 03.01. West Conshohocken, PA: ASTM—American Society for Testing and Materials; (2000) 591–630.
- [32] SAS, ANSYS, Swanson Analysis Systems, Inc., Houston, Version 12.0, (2011).
- [33] Glinka, G., Development of weight functions and computer integration procedures for calculating stress intensity factors around cracks subjected to complex stress fields. *Progress Report No.1: Stress and Fatigue-Fracture Design*, Petersburg Ontario, Canada, (1996).